Sensitivity of the pressure decline curve during the minifrac to the properties of poroelastic medium

Ekaterina Lgotina, Alexey Baykin

Novosibirsk State University

Lavrentyev Institute of Hydrodynamics of SB RAS

Coupled thermo-hydro-mechanical problems of fracture mechanics

Novosibirsk, Russia

July 1–5, 2019

Contents

1. Model extension for the case of partially saturated medium
2. Sensitivity analysis of the pressure decline curve (PDC) to the variation of the properties of medium
3. The optimization algorithm for minifrac interpretation

Part I

The hydraulic fracturing model that takes into account partial water saturation of the medium pores

Problem Formulation

Biot's equations of poroelastisity

$$\operatorname{div}\tau = 0, \quad \tau = \underbrace{\lambda \operatorname{div}\vec{u}\,\mathrm{I} + 2\mu\,\mathcal{E}(\vec{u})}_{\text{Elastic Stress}} - \underbrace{\alpha S_w p\,\mathrm{I}}_{\text{Pore Pressure}}$$

$$S_e \frac{\partial p}{\partial t} = \operatorname{div}\left(\frac{k_r}{\eta_r} k_{rw} \nabla p - \alpha S_w \frac{\partial \vec{u}}{\partial t}\right)$$

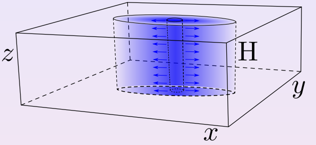

$$\mathbf{\Gamma_R}, \mathbf{\Gamma_T} : p = p_\infty, \quad \tau\langle\vec{n}\rangle = -\sigma_\infty\, \vec{e_2}$$

$$\mathbf{\Gamma_s} : u_y = 0, \quad v = 0, \quad p_y = 0$$

$$\mathbf{\Gamma_L} : v_x = 0, \quad u = 0, \quad p_x = 0$$

$$\mathbf{\Gamma_f} : \tau\langle\vec{n}\rangle = -S_w\, p\,\vec{n}, \quad v \geqslant 0$$

$$\mathbf{\Gamma_f} : \frac{\partial v}{\partial t} = \frac{\partial}{\partial x}\left(k_{rw} \frac{v^3}{3\eta_f} \frac{\partial p}{\partial x}\right) + \frac{k_r}{\eta_r} \frac{\partial p}{\partial y}$$

$$-k_{rw} \frac{v^3}{3\eta_f} \frac{\partial p}{\partial x}\bigg|_{x=0+} = Q(t)$$

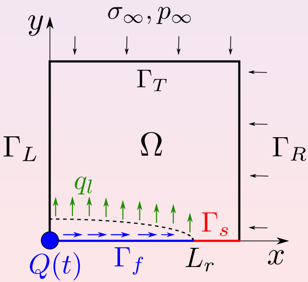

Reservoir hydraulic properties

The storativity coefficient

$$S_\varepsilon = \frac{(\alpha - \phi_0) S_w}{K_s} \left(S_w - p_w \frac{\partial S_w}{\partial p_c} \right) + \frac{\phi_0 S_w}{K_w} - \phi_0 \frac{\partial S_w}{\partial p_c},$$

The ***van Genuchten-Mualem*** (VGM) model

$$S_w = S_{rw} + (1 - S_{rw}) \left[1 + \left(\frac{p_c}{p_{ref}} \right)^{1/(1-m)} \right],$$

$$k_{rw} = (S_e)^{1/2} \left[1 - \left(1 - S_e^{1/m} \right)^m \right]^2,$$

$$S_e = (S_w - S_{rw})/(1 - S_{rw}).$$

Solution Method: Weak Formulation

$$\int_\Omega \left(\lambda \operatorname{div}(\vec{u}) - \alpha\, S_w\, p\right) \operatorname{div}(\vec{\psi}) + 2\mu\, \mathcal{E}(\vec{u}) : \mathcal{E}(\vec{\psi})\, dxdy - \int_{\Gamma_f} (S_w\, p - \sigma_{coh})\psi_2\, dx + \int_{\Gamma_T} \sigma_\infty \psi_2\, dx = 0,$$

$$\int_\Omega S_e \frac{\partial \mathbf{p}}{\partial \mathbf{t}} \varphi\, dxdy + \int_\Omega \frac{k_r}{\eta_r} k_{rw} \nabla p \cdot \nabla \varphi\, dxdy + \int_\Omega \alpha\, S_w\, \frac{\partial}{\partial t}\left(\operatorname{div} \vec{u}\right) \varphi\, dxdy + + \int_{\Gamma_f} S_w \frac{\partial \mathbf{v}}{\partial \mathbf{t}} \varphi\, dx + \int_{\Gamma_f} \frac{\mathbf{v^3}}{3\eta_f} S_w\, p_x \varphi_x\, dx - \mathbf{Q}(\mathbf{t})\varphi(0,0) = 0$$

$$\Gamma_s : \quad \psi_2 = 0, \quad v = 0$$
$$\Gamma_R : \quad \varphi = 0, \quad p = 0$$

Solve via
Finite Element Method

* *Golovin S. V., Baykin A. N.* **Influence of pore pressure on the development of a hydraulic fracture in poroelastic medium of the reservoir.** // Accepted in Int. J. Rock Mech. Min.

Cohesive law

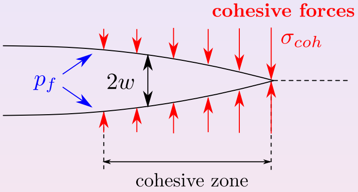

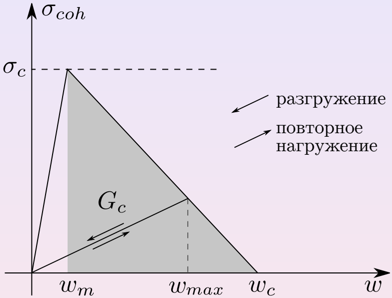

K. Park, G. H. Paulino, **Computational implementation of the PPR potential-based cohesive model in ABAQUS: Educational perspective**, 2012.

Simulation Parameters

Parameter	Value
Domain size R_x, R_y	0.25 m, 0.125 m
Young's Modulus, E	17 GPa
Poisson's Ratio, ν	0.2
Fracture Energy, G_c	120 Pa·m
Critical Cohesive Stress, σ_c	1.25 MPa
Reservoir Permeability, k_r	10^{-14} m^2
Biot Coefficient, α	1
Closure Stress, σ_∞	3 MPa
Reservoir Fluid Viscosity, η_r	10^{-3} Pa $\cdot$ sec
Fracture Fluid Viscosity, η_f	10^{-3} Pa $\cdot$ sec
Rate per Unit Height, $2Q_0$	8×10^{-4} m^3/sec
Initial Degree of Saturation, S_{w0}	**0.899**
Residual Degree of Saturation, S_{rw}	0
Empirical Curve-fitting Parameter, m	0.4396
Reference Pressure, p_{ref}	18.6 MPa
Bulk Modulus of Solid Phase, K_s	13.46 GPa
Bulk Modulus of Wetting Phase, K_w	0.2 GPa

Verification

Test 1. Single fluid injection:

$$Q(t) = Q_{single}(t) = \begin{cases} Q_0, & 0 \leqslant t < 0.625, \\ 0, & 0.625 \leqslant t \leqslant 1. \end{cases}$$

Test 2. Sequence of fluid injections:

$t \in [t_i, t_{i+1})$	$Q(t)$
$[0, 0.2)$	Q_0
$[0.2, 0.2669)$	0
$[0.2669, 0.4739)$	Q_0
$[0.4739, 0.5915)$	0
$[0.5915, 0.7995)$	Q_0
$[0.7995, 0.96)$	0
$[0.96, 1.161)$	Q_0
$[1.161, 1.362)$	0

$t \in [t_i, t_{i+1})$	$Q(t)$
$[1.362, 1.567)$	Q_0
$[1.567, 1.796)$	0
$[1.796, 2.01)$	Q_0
$[2.01, 2.275)$	0
$[2.275, 2.496)$	Q_0
$[2.496, 2.803)$	0
$[2.803, 2.971)$	Q_0
$[2.971, 3.387)$	0

* *T. Mohammadnejad, J. E. Andrade,* **Numerical modeling of hydraulic fracture propagation, closure and reopening using XFEM with application to in-situ stress estimation**, 2016.

Test 1. Pressure at wellbore

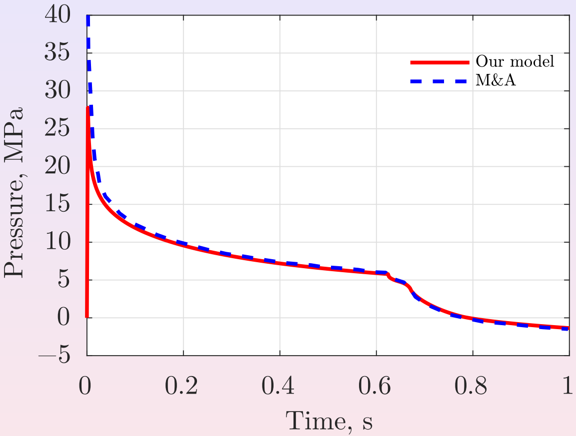

Time history of **pressure at wellbore** for single injection test Q_{single}

Test 1. Fracture geometry

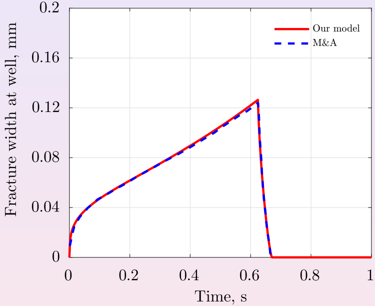

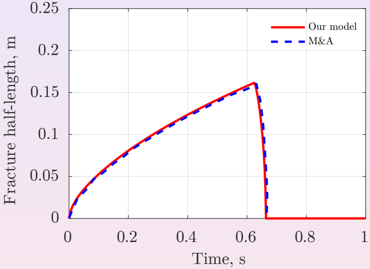

Time histories of fracture **width at wellbore** and fracture **half-length** for single injection test $Q_{single}(t)$

Test 2. Pressure at wellbore

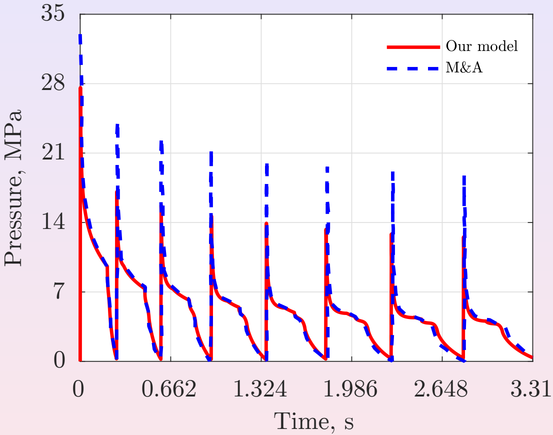

Pressure at wellbore in case of multiple injections $Q_{multiple}$

Test 2. Fracture geometry

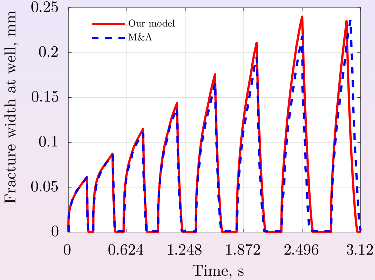

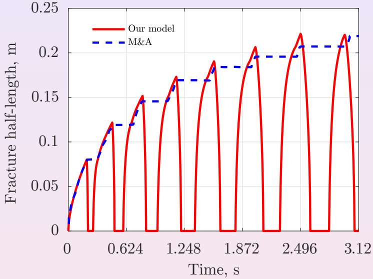

Time histories of fracture **width at wellbore** and fracture **half-length** in case of multiple injections $Q_{multiple}(t)$

Boundary numerical effect

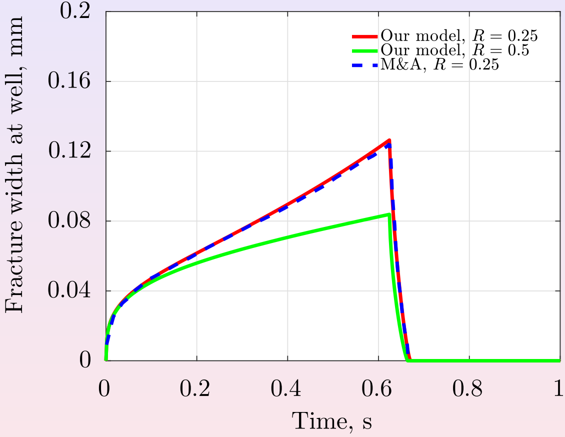

Part II

Interpretation of the PDC taking into account poroelastic effects

Sensitivity analysis: parameters

Parameter	Value
Domain size R $(R_x = R_y)$	45 m
Young's Modulus, E	17 GPa
Poisson's Ratio, ν	0.2
Fracture Energy, G_c	120 Pa·m
Critical Cohesive Stress, σ_c	1.25 MPa
Biot Coefficient, α	0.75
Reservoir Fluid Viscosity, η_r	10^{-3} Pa $\cdot$ sec
Fracture Fluid Viscosity, η_f	10^{-3} Pa $\cdot$ sec
Rate per Unit Height, $2Q_0$	10^{-3} m^2/sec
Reservoir Pressure, p_∞	**0** MPa
Initial Degree of Saturation, S_{w0}	**1**

Permeability influence on pressure curve

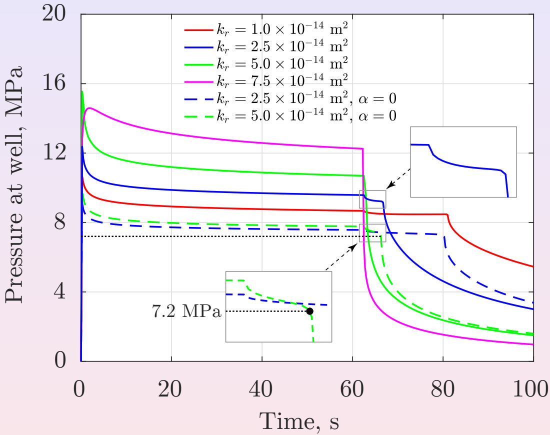

Pressure at wellbore for different permeability values in coupled ($\alpha = 0.75$) and uncoupled ($\alpha = 0$) cases

Permeability influence on fracture size

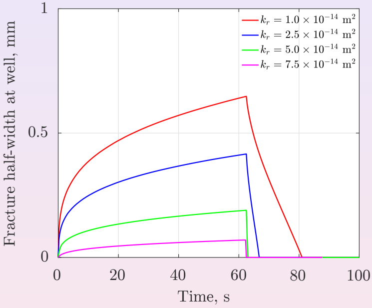

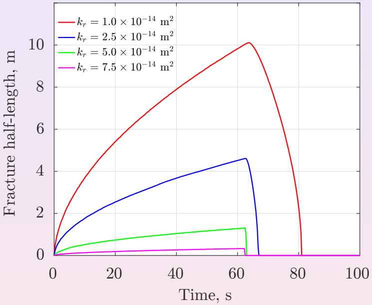

Fracture **half-width at wellbore** and **half-length** for different permeability values

Closure stress influence on pressure curve

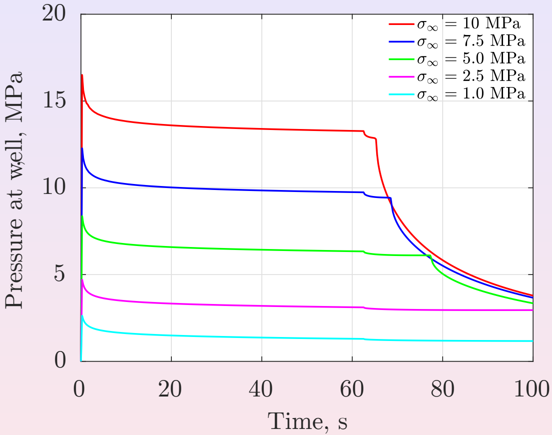

Pressure at wellbore for different closure stress values

Closure stress influence on fracture size

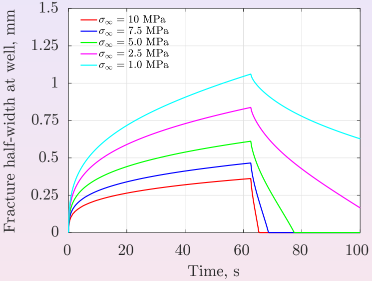

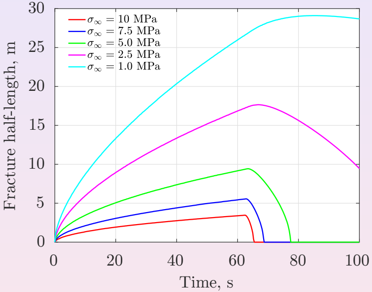

Fracture **half-width at wellbore** and **half-length** for different closure stress values

Saturation INFLUENCE ON PRESSURE CURVE

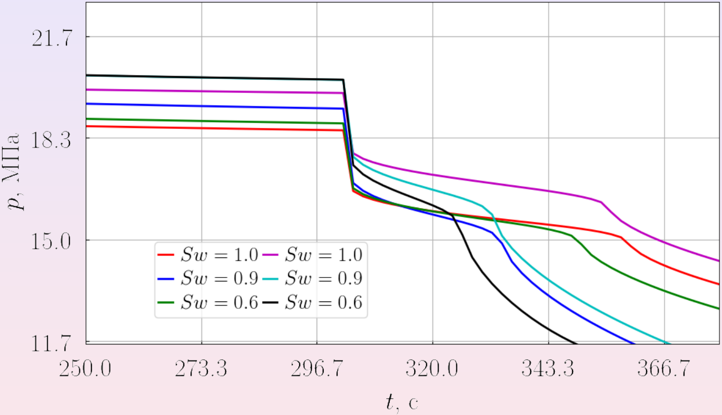

Sensitivity analysis of the PDC to **Biot's coefficient** ($\alpha = 0, 0.75$) for different permeability

Walls' **asperity** influence

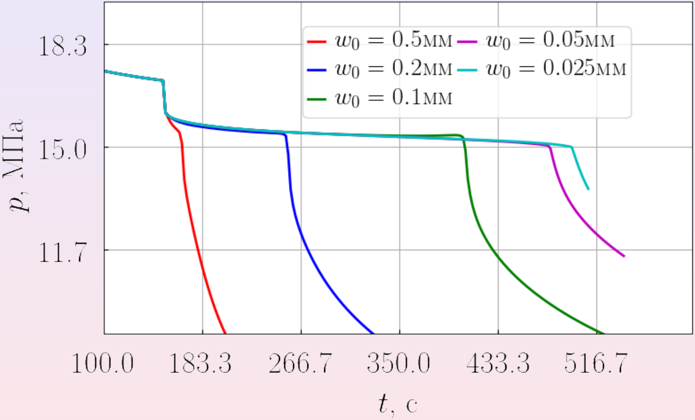

Sensitivity analysis of the PDC to **residual half-aperture**

Stiffness INFLUENCE

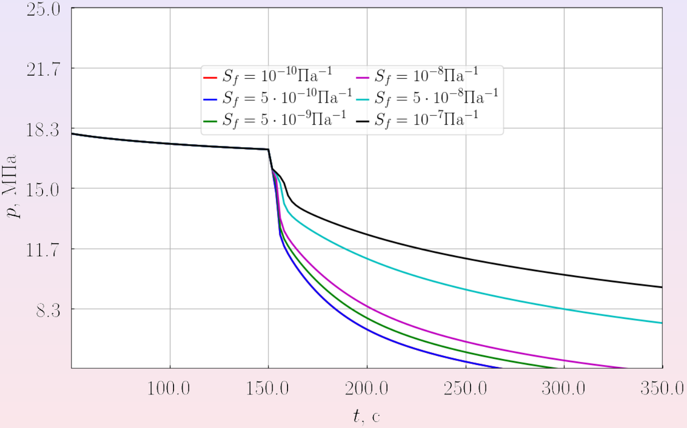

Sensitivity analysis of the PDC to fracture **stiffness** ($w_0 = 0.2\ mm$)

Radial HF Poroelastic Model

$$\operatorname{div}\tau = 0, \quad \tau = \lambda \operatorname{div}\vec{u}\,\mathrm{I} + 2\mu\,\mathcal{E}(\vec{u}) - \alpha p\,\mathrm{I}$$
$$S_e \frac{\partial p}{\partial t} = \operatorname{div}\left(\frac{k_r}{\eta_r}\nabla p - \alpha\frac{\partial \vec{u}}{\partial t}\right)$$

$$\mathbf{\Gamma_R}, \mathbf{\Gamma_T} : p = p_\infty, \quad \tau\langle\vec{n}\rangle = -\sigma_\infty\,\vec{e_2}$$
$$\mathbf{\Gamma_f} : \vec{n}\cdot\tau\langle\vec{n}\rangle = -p + \sigma_0 + \sigma_{coh}, \quad s\cdot\tau\langle\vec{n}\rangle = 0$$
$$\mathbf{\Gamma_f} : \frac{\partial w}{\partial t} = \frac{1}{r}\frac{\partial}{\partial r}\left(r\frac{w^3}{3\eta_f}\frac{\partial p}{\partial r}\right) + \frac{k_r}{\eta_r}\frac{\partial p}{\partial z}$$
$$Q_{bot}(t) = \lim_{|C|\to 0}\int_C \mathbf{q_f}\cdot\vec{n}dl, \quad \mathbf{q_f} = -\frac{2w^3}{3\eta_f}\frac{\partial p}{\partial r}$$

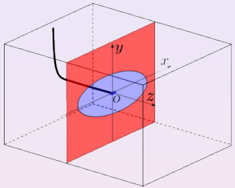

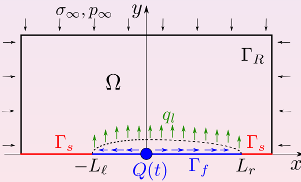

Wellbore Influence

$$Q_{bot} = \frac{\rho_{top}}{\rho_{bot}}Q_{top} - V_w\,c_w\frac{\partial p_w}{\partial t}, \quad p_w = p$$

Wellbore influence

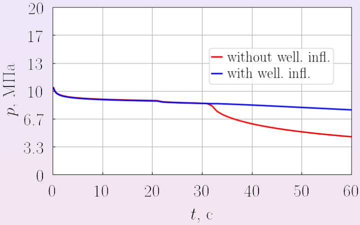

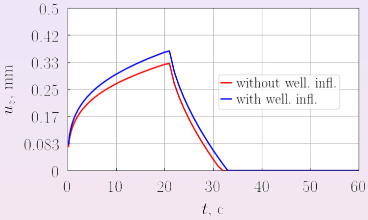

Pressure at wellbore and half-width in cases **with** and **without** wellbore influence

Optimizer

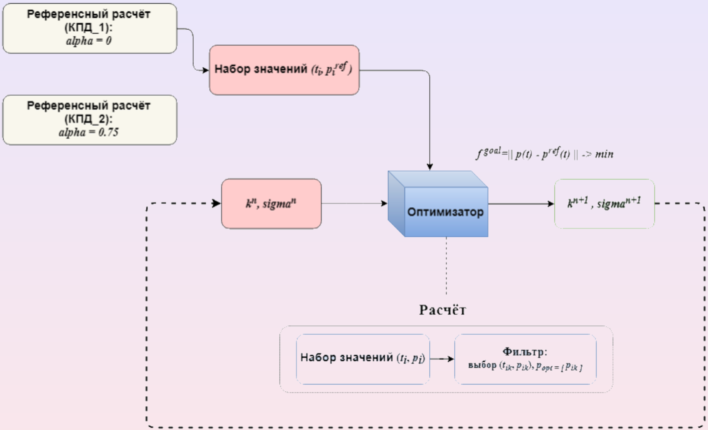

Optimization algorithm

THE TESTING OF METHOD

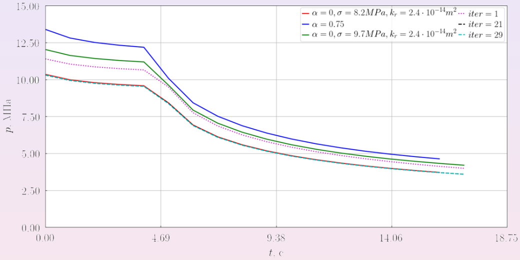

f_{goal} : **red** curve (PDC^{ref})
$\sigma_{ref} = 8.2\ MPa$
$k_{ref} = 2.4 \cdot 10^{-14}\ m^2$

Initial guess:
$\sigma_0 = 9.7\ MPa$
$k_0 = 2.4 \cdot 10^{-14}\ m^2$

Result:

$\sigma_{opt} = 8.164\ MPa$

$k_{opt} = 2.359 \cdot 10^{-14}\ m^2$

The result of optimization

The testing of method ($\alpha = 0.75$)

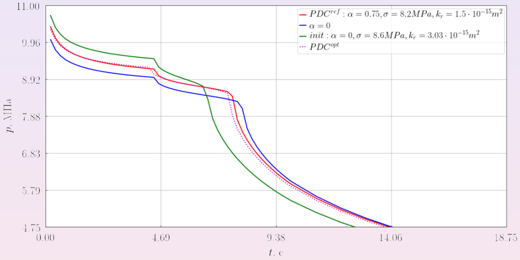

f_{goal} : **red** curve (PDC^{ref})
$\sigma_{ref} = 8.2\ MPa$
$k_{ref} = 1.5 \cdot 10^{-15}\ m^2$

Initial guess:
$\sigma_0 = 9.7\ MPa$
$k_0 = 3.03 \cdot 10^{-15}\ m^2$

Result:

$\sigma_{opt} = 8.459\ MPa$

$k_{opt} = 1.54 \cdot 10^{-15}\ m^2$

The result of optimization

Results

1. The model of a hydraulic fracture in a partially saturated poroelastic medium is constructed
2. The comparison with analogous model (by foreign authors) has been made “Numerical modeling of hydraulic fracture propagation, closure and reopening using XFEM with application to in-situ stress estimation” (Mohammadnejad, Andrade, 2016).
3. The sensitivity analysis of the PDC to reservoir parameters according to the results of numerical simulation shows the presence of the characteristic features of the curve and shows the significant influence of the effects of poroelasticity on its characteristics
4. The obtained results serve as a basis for a further development of the more accurate methods for a minifrac data interpretation

Results

1. The model of a hydraulic fracture in a partially saturated poroelastic medium is constructed
2. The comparison with analogous model (by foreign authors) has been made "Numerical modeling of hydraulic fracture propagation, closure and reopening using XFEM with application to in-situ stress estimation" (Mohammadnejad, Andrade, 2016).
3. The sensitivity analysis of the PDC to reservoir parameters according to the results of numerical simulation shows the presence of the characteristic features of the curve and shows the significant influence of the effects of poroelasticity on its characteristics
4. The obtained results serve as a basis for a further development of the more accurate methods for a minifrac data interpretation

Results

1. The model of a hydraulic fracture in a partially saturated poroelastic medium is constructed
2. The comparison with analogous model (by foreign authors) has been made “Numerical modeling of hydraulic fracture propagation, closure and reopening using XFEM with application to in-situ stress estimation” (Mohammadnejad, Andrade, 2016).
3. The sensitivity analysis of the PDC to reservoir parameters according to the results of numerical simulation shows the presence of the characteristic features of the curve and shows the significant influence of the effects of poroelasticity on its characteristics
4. The obtained results serve as a basis for a further development of the more accurate methods for a minifrac data interpretation

Results

1. The model of a hydraulic fracture in a partially saturated poroelastic medium is constructed
2. The comparison with analogous model (by foreign authors) has been made "Numerical modeling of hydraulic fracture propagation, closure and reopening using XFEM with application to in-situ stress estimation" (Mohammadnejad, Andrade, 2016).
3. The sensitivity analysis of the PDC to reservoir parameters according to the results of numerical simulation shows the presence of the characteristic features of the curve and shows the significant influence of the effects of poroelasticity on its characteristics
4. The obtained results serve as a basis for a further development of the more accurate methods for a minifrac data interpretation

Further work

Minifrac interpretation within the poroelastic model:

1. to obtain the fast method of correction of the closure pressure
2. correct calibration of geomechanics
3. matching with field data

Further work

Minifrac interpretation within the poroelastic model:

1. to obtain the fast method of correction of the closure pressure
2. correct calibration of geomechanics
3. matching with field data

Further work

Minifrac interpretation within the poroelastic model:

1. to obtain the fast method of correction of the closure pressure
2. correct calibration of geomechanics
3. matching with field data

Thank you
for your
attention!